

Multi-hazard risk assessment for roads: Probabilistic versus deterministic approaches

Stefan Oberndorfer^{1,2}, Philip Sander³, Sven Fuchs²

¹Chartered Engineering Consultant for Mountain Risk Engineering and Risk Management, Ecking 57, 5771 Leogang, Austria

²Institute of Mountain Risk Engineering, University of Natural Resources and Life Sciences, Peter Jordan Straße 82, 1190 Vienna, Austria

³Institute of Construction Management, Bundeswehr University Munich, Werner-Heisenberg-Weg 39, 85577 Neubiberg, Germany

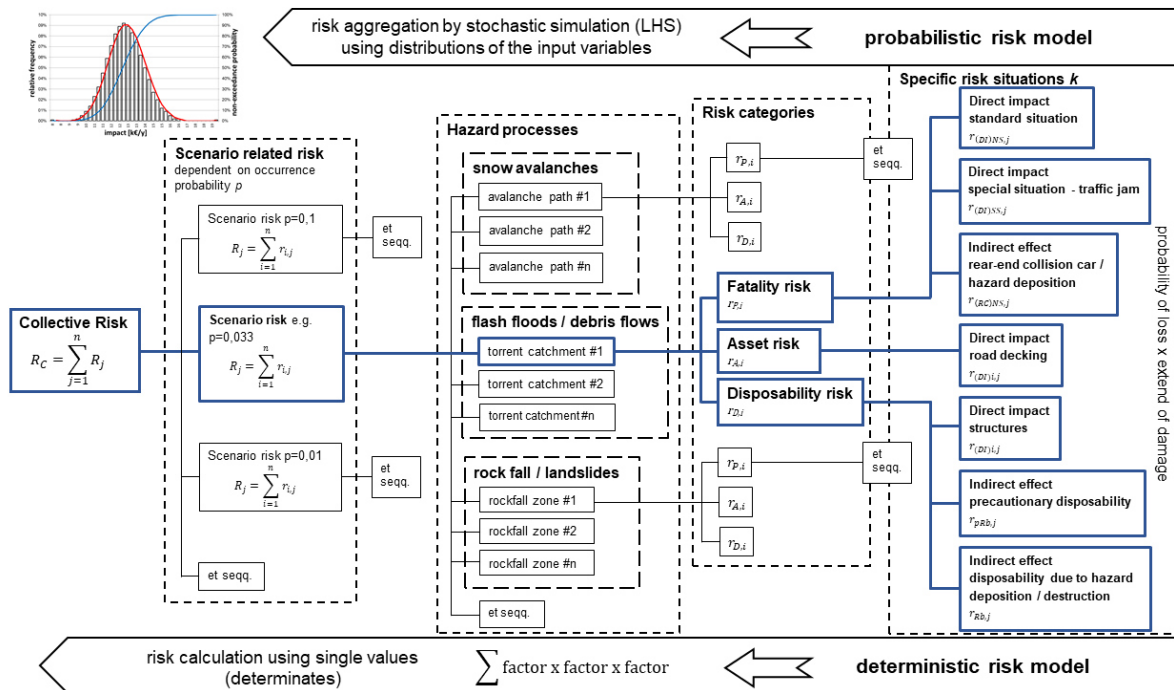
Correspondence to: Stefan Oberndorfer (office@oberndorfer-zt.at)

Abstract. Mountain hazard risk analysis for transport infrastructure is regularly based on deterministic approaches. Standard risk assessment approaches for roads need a variety of variables and data for risk computation, however without considering potential uncertainty in the input data. Consequently, input data needed for risk assessment is normally processed as discrete mean values without scatter, or as an individual deterministic value from expert judgement if no statistical data is available. To overcome this gap, we used a probabilistic approach to analyse the effect of input data uncertainty on the results, taking a mountain road in the Eastern European Alps as case study. The uncertainty of the input data is expressed with potential bandwidths using two different distribution functions. The risk assessment included risk for persons, property risk and risk for non-operational availability exposed to a multi-hazard environment (torrent processes, snow avalanches, rock fall). The study focuses on the epistemic uncertainty of the risk terms (exposure situations, vulnerability factors, monetary values) ignoring potential sources of variation in the hazard analysis. As a result, reliable quantiles of the calculated probability density distributions attributed to the aggregated road risk due to the impact of multiple-mountain hazards were compared to the deterministic outcome from the standard guidelines on road safety. The results based on our case study demonstrate that with common deterministic approaches risk might be underestimated in comparison to a probabilistic risk modelling setup, mainly due to epistemic uncertainties of the input data. The study provides added value to further develop standardized road safety guidelines and may therefore be of particular importance for road authorities and political decision-makers.

1 Introduction

Mountain roads are particularly prone to natural hazards, and consequently, risk assessment for road infrastructure focused on a range of different hazard processes, such as landslides (Benn, 2005; Schögl et al., 2019), rockfall (Bunce et al., 1997; Hungr and Beckie, 1998; Roberds, 2005; Ferlisi et al., 2012; Michoud et al., 2012; Unterrader et al., 2018) and snow avalanches (Schaerer, 1989; Kristensen et al., 2003; Margreth et al., 2003; Zischg et al., 2005; Hendrikx and Owens, 2008; Rheinberger et al., 2009; Wastl et al., 2011). These studies have in common that they exclusively address the interaction of individual hazards with values at risk of the built environment and/or of society and use qualitative, semi-quantitative and/or quantitative approaches. However, there is still a gap in multi-hazard

36 risk assessments for road infrastructure. The article provides a comparison of a standard (deterministic) risk
 37 assessment approach for road infrastructure exposed to a multi-hazard environment with a probabilistic risk analysis
 38 method to show the potential bias in the results. The multi-hazard scope of the study is based on a spatially-oriented
 39 approach to include all relevant hazards within our study area. Using this approach, we address the consequences of
 40 multiple hazard impact on road infrastructure and compare the monetary loss of the different hazard types. The
 41 standard framework from ASTRA (2012) for road risk assessment is based on a deterministic approach and
 42 computes road risk based on a variety of input variables. Data is generally addressed with single values without
 43 considering potential input data uncertainty. We used this standardized framework for operational risk assessment for
 44 roads and transportation networks and supplemented this well-established deterministic method with a probabilistic
 45 framework for risk calculation (Fig. 1). A probabilistic approach enables the quantification of epistemic uncertainty
 46 and uses probability distributions to characterize data uncertainty of the input variables while a deterministic
 47 computation uses single values with discrete values without uncertainty representation. While the former calculates
 48 risk with constant or discrete values, ignoring the epistemic uncertainty of the variables, the latter enables the
 49 consideration of the potential range of parameter value by using different distributions to characterize the input data
 50 uncertainty. Our study focuses on the epistemic uncertainty of the risk terms (exposure situations, vulnerability
 51 factors, monetary values) ignoring potential sources of variation within hazard analysis. Thus, the probability of
 52 occurrence of the hazard event was not assessed in a probabilistic way. Since deriving the likelihood of occurrence as
 53 part of the hazard analysis is crucial for risk analysis, a high source of uncertainty is attributed to this factor (Schaub
 54 and Bründl, 2010).



55
 56 **Figure 1.** Exemplified flow chart for the risk assessment method following the standard approach (deterministic risk
 57 model) from ASTRA (2012) which was supplemented with the probabilistic risk model in present study. In the
 58 deterministic approach each risk variable is addressed with single values and the specific risk situations are summed
 59 up to risk categories for each hazard process class and scenario (probability of occurrence of the hazard process) and

60 finally to the collective risk, whereas the probabilistic setup uses a probability distributions to characterize each risk
61 variable and further aggregates risk by stochastic simulation to the total risk.

62 **2 Background**

63 **2.1 Multi-hazard risk assessment**

64 According to Kappes et al. (2012a), two approaches to multi-hazard risk analysis can be distinguished, a spatially-
65 oriented and a thematically-defined method. While the first aims to include all relevant hazards and associated loss in
66 an area, the latter deals with the influence or interaction of one hazard process on another hazard, frequently
67 addressed as hazards chain or cascading hazards, meaning that the occurrence of one hazard is triggering one or
68 several second-order (successive) hazards. One of the major issues in multi-hazard risk analysis – see Kappes et al.
69 (2012a) for a comprehensive overview – lies in the different process characteristics which lead to challenges for a
70 sound comparison of the resulting risk level among different hazard types due to different reference units.
71 Standardization by a classification scheme for frequency and intensity thresholds of different hazard types resulting
72 in semi-quantitative classes or ranges allows for a comparison among different hazard types, such as shown in
73 Table 2. Therefore, the analysis of risk for transport infrastructure is often focused on an assessment of different
74 hazard types affecting a defined road section rather than on hazard chains or cascades (Schlögl et al., 2019).
75 Following this approach, hazard-specific vulnerability can be assessed either in terms of loss estimates (e.g.,
76 Papathoma-Köhle et al., 2011; Fuchs et al., 2019) or in terms of other socioeconomic variables, such as limited
77 access in case of road blockage or interruption (Schlögl et al., 2019). Focusing on the first and neglecting any type of
78 hazard chains, our study demonstrates the application of risk to a specific road section in the Eastern European Alps
79 and shows the sensitivity of the results using deterministic and probabilistic risk approaches.

80 **2.2 Deterministic risk concept**

81 Quantitative risk analyses for natural hazards are regularly based on deterministic approaches, and the temporal and
82 spatial occurrence probability of a hazard process with a given magnitude is multiplied by the expected
83 consequences, the latter defined by values at risk times vulnerability (Varnes, 1984; International Organisation for
84 Standardisation, 2009). A universal definition of risk relates the likelihood of an event with the expected
85 consequences, thus manifests risk as a function of hazard times consequences (UNISDR, 2004; ISO, 2009).
86 Depending on the spatial and temporal scale, values at risk include exposed elements, such as buildings (Fuchs et al.,
87 2015, 2017), infrastructure systems (Guikema et al., 2015) and people at risk (Fuchs et al., 2013). These elements at
88 risk are linked to potential loss using vulnerability functions, indices or indicators (Papathoma-Köhle, 2017), and can
89 be expressed in terms of direct and indirect, as well as tangible and intangible loss (Markantonis et al., 2012; Meyer
90 et al., 2013). While direct loss occurs immediately due to the physical impact of the hazard, indirect loss occurs with
91 a certain time lag after an event (Merz et al., 2004, 2010). Furthermore, the distinction between tangible or intangible
92 loss is depending on whether or not the consequences can be assessed in monetary terms. In this context,
93 vulnerability is defined as the degree of loss given to an element of risk as a result from the occurrence of a natural
94 phenomenon of a given intensity, ranging between 0 (no damage) and 1 (total loss) (UNDRO, 1979; Fell et al., 2008;
95 Fuchs, 2009). This definition highlights a physical approach to vulnerability within the domain of natural sciences,

96 neglecting any societal dimension of risk. However, the expression of vulnerability due to the impact of a threat on
97 the element at risk considerably differs among hazard types (Papathoma-Köhle et al., 2011).
98 Using a deterministic approach, the calculation of risk has repeatedly been conceptualised by Eq. (1) (e.g. Fuchs et
99 al. 2007; Oberndorfer et al. 2007; Bründl et al. 2009) and is dependent on a variety of variables all of which being
100 subject to uncertainties (Grêt-Regamey and Straub, 2006).

$$101 \quad R_{i,j} = f(p_j, p_{i,j}, A_i, v_{i,j}) \quad (1)$$

102 Where $R_{i,j}$ = risk dependent of object i and scenario j ; p_j = probability of defined scenario j ; $p_{i,j}$ probability of
103 exposure of object i to scenario j ; A_i = value of the object i (the value at risk affected by scenario j); $v_{i,j}$ =
104 vulnerability of the object i in dependence on scenario j .

105 With respect to mountain hazard risk assessment, standardised approaches are available, such as IUGS (1997), Dai et
106 al. (2002), Bell and Glade (2004), and Fell et al. (2008a, b) for landslides, Bründl et al. (2010) for snow avalanches,
107 and Bründl (2009) or ASTRA (2012) for a multi-hazard environment. These approaches, however, usually neglect
108 the inherent uncertainties of involved variables. In particular, they ignore the probability distributions of the variables
109 (Grêt-Regamey and Straub, 2006) by obtaining the results with constant input parameters, which may lead to bias
110 (over- and underestimation dependent on the scale of input variables) in the results. Therefore, loss assessment for
111 natural hazard risk is associated with high uncertainty (Špačková et al., 2014 and Špačková, 2016) and studies
112 quantifying uncertainties of the expected consequences are underrepresented (Grêt-Regamey and Straub, 2006),
113 especially regarding natural hazards impacts on roads (Schlögl et al., 2019). For the assessment of an optimal
114 mitigation strategy for an avalanche-prone road Rheinberger et al. (2009) considers parameter uncertainty by
115 assuming a joint (symmetric) deviation of $\pm 5\%$ for all input values to construct a confidence interval for the baseline
116 risk. The assessment of uncertainty of natural hazard risk is therefore frequently represented by sensitivity analyses
117 to show the sensitivity through a shift in input values on the results. Thus, the use of confidence intervals allows a
118 discrete calculation of risk with different model setups. In our study, we quantify the potential uncertainties within
119 road risk assessment using a stochastic risk assessment approach under consideration of the probability distribution
120 of input data.

121 **2.3 Uncertainties within risk assessment**

122 Since the computation of risk for roads requires a variety of auxiliary calculations, a broad range of input data are
123 used, such as the spatial and temporal probability of occurrence of specific design events. These auxiliary
124 calculations subsequently provide variables necessary for risk computation of the respective system under
125 investigation. Individual contributing variables are often characterized either as mean value of the potential spectrum
126 from a statistical dataset or, as a consequence of incomplete data, as a single value from expert judgement. Expert
127 information is frequently processed with semi-quantitative probability classes and therefore subjected to considerable
128 uncertainties. Consequently, they serve as rough qualitative appraisals encompassing a high degree of uncertainty.

129 The use of vulnerability parameters or lethality values as a function of process-specific intensities is often based on
130 incomplete or insufficient statistical data resulting from missing event documentation (Fuchs et al., 2013). As
131 discussed in Kappes et al. (2012a), Papathoma-Köhle et al. (2011, 2017) and Ciurean et al. (2017) with respect to
132 mountain hazards, potential sources of uncertainty in vulnerability assessment are independent of the applied

133 assessment method. The amplitude in data is considerably high in continuous vulnerability curves or functions, but
134 also in discrete (minimum and maximum) vulnerability values referred to as matrices (coefficients), and in indicator-
135 /index-based methods used to calculate the cumulative probability of loss. With regard to the uncertainty in
136 vulnerability matrices, Ciurean et al. (2017) suggested a fully probabilistic simulation in order to quantify the
137 propagation of errors between the different stages of analysis by substituting the range of minimum-maximum values
138 with a probability distribution for each variable in the model.

139 Grêt-Regamey and Straub (2006) listed potential sources of uncertainties in risk assessment models and classified
140 uncertainties into aleatory and epistemic uncertainties. The first is considered as inherent to a system associated to
141 the natural variability over space and time (Winter et al., 2018) and the variability of underlying random or stochastic
142 processes (Merz and Thieken, 2005, 2009), which cannot be further reduced by an increase in knowledge,
143 information or data. The latter results from incomplete knowledge and can be reduced with an increase of cognition
144 or better information of the system under investigation (Merz and Thieken, 2004, 2009; Grêt-Regamey and Straub,
145 2006). Particularly referring to deterministic risk analysis, epistemic uncertainty is associated with a lack of
146 knowledge about quantities of fixed but poorly known values (Merz and Thieken, 2009). Špačková (2016) pointed
147 out the importance of interactions (correlations) between uncertainties which may affect the final results, an issue
148 that was also discussed in the framework of multi-hazard risk assessments (Kappes, 2012a, b). Therefore,
149 uncertainties should be included in the analysis by their upper and lower credible limits or by integrating confidence
150 intervals reflecting the incertitude of input data, for an in-depth discussion see e.g. Apel et al. (2004), Merz and
151 Thieken (2004, 2009), Bründl et al. (2009) and Winter et al. (2018).

152 **2.4 Deterministic vs. probabilistic risk**

153 Deterministic and probabilistic methods for risk analysis differ significantly in approach. Deterministic methods
154 generally use a defined value (point value) for probability and for the impact (consequence) and consider risk by
155 multiplying the probability of occurrence with the potential consequences. The result is an “expected value” of risk.
156 If multiple risks e.g. with varying frequencies are addressed, the total risk is expressed as the simple sum of single
157 risks resulting in an expected annual average loss. However, information about probability or best and/or worst-case
158 scenarios are often excluded. In particular, the following shortcomings of deterministic approaches can be
159 summarized (Tecklenburg 2003), which in turn leads us to a recommendation of probability-based risk approaches:

- 160 - A deterministic method gives equal weight to those risks that have a low probability of occurrence and high
161 impact and to those risks that have a high probability of occurrence and low impact by using a simple
162 multiplication of probability and impact, a topic which is also known as risk aversion effect and is
163 controversially discussed in the literature (e.g., Wachinger et al, 2013; Lechowska, 2018).
- 164 - By multiplying the two elements of probability and impact, these values are no longer independent.
165 Therefore, this method is not adequate for aggregation of risks where both probability and impact information
166 need to remain available. Due to multiplication, the only information that remains is the mean value.
- 167 - The actual impact will definitely deviate from the deterministic value (i.e., the mean).
- 168 - Without the Value at Risk (VaR) information, there is no way to determine how reliable the mean value is and
169 how likely it might be exceeded. The VaR is a measure of risk in economics and describes the probability of

170 loss within a time unit, which is expressed as a specified quantile of the loss distribution (Cottin and Döhler,
171 2013).

172 In this context, deterministic systems are perfectly predictable, and the state of the parameters to describe the system
173 behaviour are fixed (single) values associated with total determinization following an entirely known rule, whereas
174 probabilistic systems include some degree of uncertainty and the variables/parameters to describe the state of the
175 system are therefore random (Kirchsteiger, 1999). The variables/parameters in probabilistic systems are described
176 with probability distributions due to incomplete knowledge, rather than with a discrete single or point value which is
177 assumed to be totally certain. Probabilistic risk modelling uses stochastic simulation with a defined distribution
178 function to generate random results within the setting of the boundary conditions. The deterministic variable is
179 usually included within the input distribution. In Table 1 the two different methods are compared.

180 **Table 1.** Deterministic versus probabilistic method for risk analysis adjusted and compiled from Sander et al. (2015)
181 and Kirchsteiger (1999).

	Deterministic method	Probabilistic method
Input	Definition of a single number for consequence as descriptive statements including conservative assumptions expressed by the probability of occurrence multiplied by the impact of the particular hazard.	The probabilistic assessment of risk requires at least one number or – for an entirely probabilistic modelling – a PDF for the probability of occurrence and several values for the impact (e.g., minimum, most likely and maximum) expressed as distribution functions, therefore including uncertainty.
Result	A simple mathematical addition to give the aggregated consequence for all risks (point value calculation). This results in an expected consequence for the aggregated risks but does not adequately represent the bandwidth (range) of the aggregated consequences. The deterministic calculation can be supplemented with upper and lower bounds (different model setups) to show the sensitivity of the input on the results using a sensitivity analysis, which are per se separate deterministic calculations.	Simulation methods e.g. Monte Carlo simulation produce a bandwidth (range) of aggregated natural hazards risks as probability distribution based on thousands of coincidental but realistic scenarios (depiction of realistic risk combinations). The method allows an explicit consideration and treatment of all types of reducible uncertainty.
Qualification	Results (monetary value or fatality per time unit) are displayed as a single sharp number, which, in itself, does not have an associated probability.	Results are displayed using probability distributions, which allow Value at Risk (VaR) interpretation for each value within the bandwidth (range).

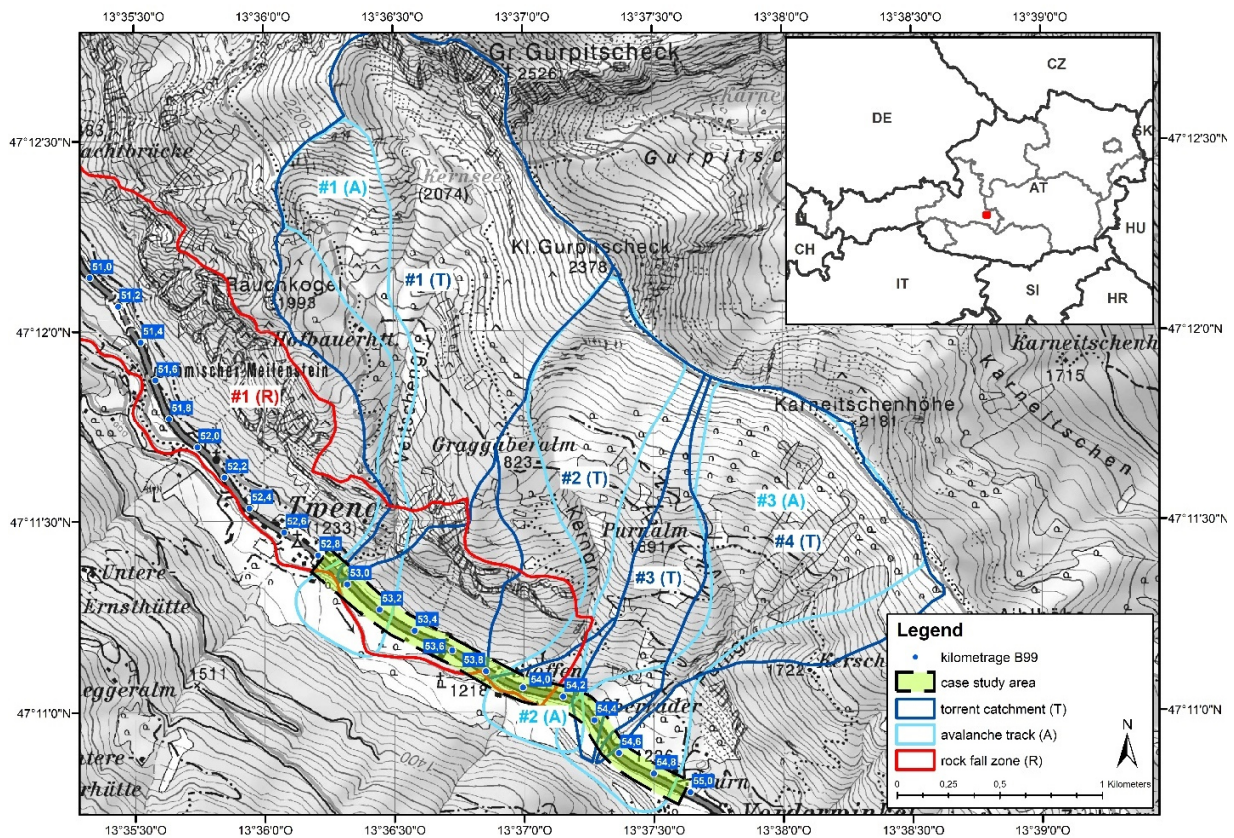
182
183 In our study we present an probabilistic design for loss calculation in order to compute the potential spectrum of
184 input data with simple distribution functions and further aggregate the intermediate data of exposure situations,
185 hazard- and scenario-related modules to the probability density function (PDF) of the total collective risk R_C by
186 means of stochastic simulation (Fig. 1). Consequently, damage induced by natural hazards impact to road
187 infrastructure as well as to traffic are represented by a range of monetary values as a prognostic distribution of the
188 expected annual average loss instead of an individual amount.

189 **3. Case study**

190 The study area is located in the Eastern European Alps, within the Federal State of Salzburg, Austria (Fig. 2). The
191 case study is a road segment of the federal highway B99 with an overall length of two kilometers ranging from
192 km 52.8 to km 54.8 and is endangered by multiple types of natural hazards. The road segment was chosen to
193 demonstrate the advantages of using probabilistic risk approaches in comparison to traditional deterministic methods.
194 The mountain road under examination is part of a north-south traverse over the main ridge of the Eastern European
195 Alps and is therefore an important regional transit route. Furthermore, the road provides access to the ski resort of
196 Obertauern.

197 As shown in Fig. 2, the road segment is affected by three avalanche paths, four torrent catchments and one rockfall
198 area. The four torrent catchments have steep alluvial fans on the valley basin. The road segment is located at the base
199 of these fans or the road is slightly notched in the torrential cone and passes the channels either with bridges or with
200 culverts. The rockfall area is situated in the western part of the road segment. Approximately two third of the study
201 area is affected from rock fall processes either as single blocks or by multiple blocks.

202 The road is frequently used for individual traffic from both sides of the alpine pass. Hence, a mean daily traffic
203 (MDT) of 3,600 cars is observed. This constant frequency represents the standard situation for the potentially
204 exposed elements at risk. However, especially in the winter months the average daily traffic can considerably
205 increase up to an amount of about 7,000 cars. Thus, the traffic data underlies short-term daily and longer-term
206 seasonal fluctuations with peaks up to the double of the mean value. The importance of dynamic risk computation
207 needed for traffic corridors was also discussed earlier by Zischg et al. (2005) and Fuchs et al. (2013) with respect to
208 the spatial-temporal shifts in elements at risk. Besides of the use as a regional transit route, the road is also a central
209 bypass for one of the main transit routes through the Eastern European Alps. Hence, any closure of this main transit
210 route (A10 Tauern motorway) results in a significant increase of daily traffic frequency up to a total of 19,650 cars.
211 The evaluation of the dataset in terms of the bandwidth of the traffic data is shown in Table A6.



212
 213 **Figure 2.** Overview of the case study area and location of the natural hazards along the road segment (Source base
 214 map: © BEV 2020 – Federal Office of Metrology and Surveying, Austria, with permission N2020/69708).

215 **4. Methods**

216 **4.1 Hazard analysis**

217 The hazard analysis was part of technical studies undertaken for the road authority of the Federal State of Salzburg
 218 (Geoconsult, 2016; Oberndorfer, 2016). The results regarding the spatial impact of the hazard processes on the
 219 elements at risk and the corresponding hazard intensities were used for the loss assessment in this research. The
 220 hazard assessment included the steps of hazard disposition analysis to detect potential hazards sources within the
 221 perimeter of the road followed by a detailed numerical hazard analysis. Therefore, these analyses considered
 222 approaches for hazard-specific impact assessment according to the engineering guidelines of e.g. Bründl (2009),
 223 ASTRA (2012) and Bründl et al. (2015) and relevant engineering standards and technical regulations (Austrian
 224 Standards Organisation, 2009, 2010, 2017). The physical impact parameters of the hazard processes were calculated
 225 using numerical simulation software, such as Flow-2D for flash floods and debris flows (Flow-2D Software, 2017),
 226 SamosAT for dense and powder snow avalanches (Sampl, 2007) and Rockyfor3D for rock fall (Dorren, 2012). The
 227 hazard analyses were executed without probabilistic calculations; thus, the generated results were integrated as
 228 constant input in the risk analysis.

229 For the multi-hazard purpose three hazard types were evaluated, (1) hydrological hazards (torrential floods, flash
 230 floods, debris flows), (2) geological hazards (rock fall, landslides), and (3) snow avalanches (dense and powder snow
 231 avalanches). For each hazard type, intensity maps for the affected road segment were computed. The intensity maps
 232 specify for a specific hazard scenario the spatial extent of a certain physical impact (e.g., pressure, velocity, or
 233 inundation depth) during a reference period (Bründl et al., 2009). In order to transfer the physical impact to object-
 234 specific vulnerability values for further use in the risk assessment, three process-specific intensity classes were
 235 distinguished (Table 2). These intensity classes were based on the underlying technical guidelines (Bründl, 2009;
 236 ASTRA, 2012; Bründl et al., 2015) and were slightly adapted to comply with the regulatory framework in Austria
 237 (Republik Österreich, 1975, 1976; BMLFUW, 2011). Table 2 represents the intensity classes which correspond to
 238 the affiliated object-specific vulnerability and lethality values (mean damage values) in Tables A7 and A8.

239 **Table 2.** Process-specific intensity classes with p = pressure, h = height (suffix h_{ws} refers to water and solids), v =
 240 velocity, d = depth and E = energy (compiled and adapted from Bründl (2009), ASTRA (2012) and Republik
 241 Österreich (1975) in conjunction with Republik Österreich (1976) and BMLFUW (2011). The low intensity class for
 242 debris flow has the same intensity indicators than for inundation because it was assumed that low intensity debris
 243 flow events have equal characteristics than hydrological processes.

Hazard type	Low intensity	Medium intensity	High intensity
Snow avalanche	$1 < p < 3 \text{ kN/m}^2$	$3 < p < 10 \text{ kN/m}^2$	$p > 10 \text{ kN/m}^2$
Inundation	$h < 0.5 \text{ m}$ or $v \times h < 0.5 \text{ m}^2/\text{s}$	$0.5 < h_{ws} < 1.5 \text{ m}$ or $0.5 < v \times h < 1.5 \text{ m}^2/\text{s}$	$h_{ws} > 1.5 \text{ m}$ or $v \times h > 1.5 \text{ m}^2/\text{s}$
Debris (bed load) deposit	$h_{ws} < 0.5 \text{ m}$ or $v \times h < 0.5 \text{ m}^2/\text{s}$	$0.5 < h_s < 0.7 \text{ m}$ or $v < 1 \text{ m/s}$	$h_s > 0.7 \text{ m}$ and $v > 1.0 \text{ m/s}$
Erosion	--	$d < 1.5 \text{ m}$ or top edge of the erosion	$d > 1.5 \text{ m}$ or top edge of the erosion
Rockfall	$E < 30 \text{ kJ}$	$30 < E < 300 \text{ kJ}$	$E > 300 \text{ kJ}$

244 To determine the intensities of individual hazard processes, two different return periods were selected, a 1-in-10-year
 245 and a 1-in-30-year event (probability of occurrence $p_{10} = 0.1$ and $p_{30} = 0.033$). All three snow avalanches can either
 246 develop as powder snow avalanches or as dense flow avalanches, depending on the meteorological and/or snowpack
 247 conditions. Due to the catchment characteristics of the torrents two different indicator processes were assigned for
 248 assessing the hazard effect, depending on the two occurrence intervals. Therefore, the occurrence interval served as a
 249 proxy for the process type since we assumed for the frequently occurring events ($p = 0.1$) the hazard type “flash
 250 floods with sediment transport” and for the medium scale recurrence intervals ($p = 0.033$) debris flow processes.

251 4.2 Standard guideline for risk assessment

252 The method to calculate road risk for our case study followed the deterministic standard framework of the ASTRA
 253 (2012) guideline for operational road risk assessment. The identification of elements at risk regarding their quantity,
 254 characteristics and value as well as their temporal and spatial variability was assessed through an exposure analysis.
 255 The assessment of the vulnerability of objects (affected road segment, culverts, bridges etc.) and the lethality of

256 persons was carried out by a consequence analysis to characterize the extent of potential losses. The finally resulting
257 collective risk R_C (Eqn. 2) as a sum of all hazard types over all object classes and scenarios – under the assumption
258 that the occurrence of the individual hazards are independent from each other – was expressed in monetary terms per
259 year as a prognostic value. R_C is therefore defined as the expected annual damage caused by certain hazards and is
260 frequently used as a risk indicator (Merz et al., 2009; Špačková et al., 2014). Hence, R_C was calculated based on
261 Eqn. (1) by summing up the partial risk over all scenarios j and objects i (Bründl et al., 2009, Bründl, 2009, ASTRA,
262 2012, Bründl et al., 2015):

$$263 \quad R_C = \sum_{j=1}^n R_{C,j} \quad (2)$$

264 Where $R_{C,j}$ = the total collective risk of scenario j and objects i , $R_{C,j} = \sum_{i=1}^n r_{i,j}$.

265 According to the ASTRA (2012) guideline, the collective risk R_C is divided into three main risk groups, (1) risk for
266 persons R_P , (2) property or asset risk R_A , and (3) risk of non-operational availability or disposability R_D .

267 4.2.1 Risk for persons R_P

268 The risk characterization for persons in terms of the direct impact of a natural hazard on cars was distinguished in a
269 standard situation for flowing traffic and a situation during a traffic jam, which was seen as specific situation leading
270 to a significant increase of potentially endangered persons. Additionally, another specific case was also included
271 representing the rear-end collision either on stagnant cars or on the process depositions on the road in case of the
272 standard situation. The probability for a rear-end collision depends on the characteristics of the road and is
273 influenced by a factor of e.g. the visual range, the winding and steepness of the road, the velocity, and traffic density
274 (ASTRA, 2012). Furthermore, an additional specific scenario was explicitly considered in the case of the road
275 closure of the main transit route (A10 Tauern motorway) due to the resulting temporal peak of the mean daily traffic.
276 The statistical mean daily traffic (MDT) was used as mean quantity of persons N_p travelling along the road
277 (Table A7).

278 In order to compute R_P , the expected annual losses of persons traveling along the road segment under a defined
279 hazard scenario j was calculated as a combination of the specific damage potential or potential damage extent of
280 persons and the damage probability of the exposure situation k for persons using the road under investigation. The
281 potential losses for persons were monetized by the cost for a statistical human life as published by the Austrian
282 Federal Ministry of Transportation, Innovation and Technology (BMVIT, 2014). The published average national
283 expenses of road accidents include materially and immaterially costs (body injury, property damage and overhead
284 expenses) of road accidents and are based on statistical evaluations of the national database as well as on the
285 willingness to pay approach for human suffering. The monetized costs for a statistical human life equal 3 M€. Thus,
286 road risk for persons was calculated with three road-specific exposure situations k (Bründl et al., 2009):

- 287 1. Direct impact of the hazard event – standard situation (Eqn. 1A; Table A1)
- 288 2. Direct impact of the hazard event – specific situation due to traffic jam (Eqn. 2A; Table A2)
- 289 3. Indirect effect – rear-end collision (Eqn. 3A; Table A3)

290 The risk variables to assess R_P are stated in Table A6 for the exposure situations and in Table A7 in the Appendix.

291 **4.2.2 Property risk R_A**

292 The property risk due to the direct impact of the hazard process on physical assets of the road infrastructure was
293 calculated for each object i and scenario j using Eqn. (4A) with Table A4 under consideration of risk variables in
294 Table A8. The damage probability was assumed to be equal to the frequency of the scenario j .

295 With respect to the potential direct tangible losses within the study area, the physical assets including e.g. the road
296 decking of the street segment, culverts and bridges were expressed by the building costs of the assets calculated from
297 a reference price per unit (Table A8). The physical assets of affected cars were not addressed as this damage type is
298 not included in the standard guideline due to the assumption of an obligatory insurance coverage. The monetized
299 costs refer to replacement costs and reconstruction costs, respectively, instead of depreciated values, which is
300 strongly recommended in risk analysis by Merz et al. (2010) due to the fact that replacement cost systematically
301 overestimates the damage. Since there is a limitation of reliable or even available data on replacement costs, the
302 usage of reconstruction costs is a pragmatic procedure to calculate damage.

303 **4.2.3 Risk due to non-operational availability R_D**

304 The risk due to non-operational availability can be generally separated into economic losses due to (1) road closure
305 after a hazard event or (2) as a result of precautionary measures for road blockage. The former addresses the
306 mandatory reconditioning of the road and interruption time is depending on the severity of the damage. For our case
307 study, only the precautionary non-operational availability was calculated with Eqn. (5A), Table A5 and variables in
308 Table A9 because the village of Obertauern can be accessed from both directions of the mountain pass road.
309 Therefore, a general accessibility of the village was supposed because it was assumed that events only lead to a road
310 closure on one site of the pass. Potential costs resulting from time delays for necessary detours or e.g. from an
311 increase of environmental or other stresses were neglected. The maximum intensity of the process served as a proxy
312 for the duration of the road closure.

313 The direct intangible costs for non-operational availability of the road were approximated from statistical data
314 accounting for the business interruption and the loss of profits of the tourism sector in the village of Obertauern due
315 to road closure (see Table A9). The village of Obertauern is a major regional tourism hot spot and therefore the
316 predominant income revenues are based on tourism, thus other business divisions were neglected. Regarding the
317 precautionary expected losses only snow avalanches were included, due to the obligatory legal implementation of a
318 monitoring of a regional avalanche commission. Thus, a reliable procedure for a road closure could be assumed.

319 **4.3 Risk computation**

320 For purpose of computing road risk, the risk Equations 1A to 5A from the standard guideline (ASTRA, 2012), stated
321 in the Appendix in conjunction with Tables A1 to A5, were used without further modification both for the
322 deterministic and for the probabilistic calculation. Hence, the probabilistic setup is based on the same equations as
323 the standard approach, but the variables were addressed with probability distributions instead of single values. In a
324 first step, the deterministic result was computed as a base value for comparison with the results (probability density
325 functions PDFs) of the two diverging probabilistic setups. In a second step, a probabilistic model was integrated into
326 the same calculation setup to consider the band width of the risk-contributing variables. Using this probabilistic

327 model, the individual risk variables were addressed with two separate probability distributions. The flow chart in
328 Fig. 1 illustrates the risk assessment method and distinguishes between the deterministic and the probabilistic risk
329 model. The diagram exemplarily demonstrates the calculation steps for both model setups. Whereas only the single
330 value of the input data was processed within the standard (deterministic) setup, the probabilistic risk model utilized
331 the bandwidth of each variable denoted in Tables A6 to A9 in the Appendix. These values were either defined from
332 statistical data, expert judgement or from existing literature. The range represents the assumed potential scatter of the
333 variables including a minimum (lower bound l), an expected or most likely value (m) and a maximum value (upper
334 bound u). The deterministic setup was calculated with the expected value, which corresponds in most cases to the
335 recommended input value of the guideline. The choice of the variable range in Tables A6 to A9 in the Appendix is
336 case study specific and cannot be transferred to other studies without careful validation.

337 4.3.1 Probabilistic framework

338 Within the probabilistic risk modelling setup, the contributing variables for computing the prognostic annual loss
339 were calculated in a stochastic way using their potential range. The probabilistic risk calculation was conducted with
340 the software package RIAAT – Risk Administration and Analysis Tool (RiskConsult, 2016). The probabilistic setup
341 comprised two different and independent calculation runs each with two different distribution functions to
342 characterize the uncertainty of the input variables. Hence, each variable was modelled using either (1) a triangular or
343 three-point distribution (TPD) or (2) a beta-PERT distribution (BPD) within the probabilistic model, which generated
344 two independent probabilistic setups and results. The discrete risk calculation with two different approaches of
345 probability distributions facilitated a comparison of the applicability and the sensitivity of the simple distribution
346 functions on the results. The expected annual monetary losses induced by the three hazard types were aggregated and
347 further compacted to the probability density function (PDF) of the total risk caused by multi-hazard impact. Finally,
348 the two different PDFs from the stochastic risk assessment were compared with the result from the deterministic
349 method to show the potential dynamics in the results.

350 1. Triangular distribution (TPD)

351 The triangular distribution derives its statistical properties from the geometry: it is defined by three parameters l for
352 lower bound, m for most likely value (the mode) and u for upper bound. Whereas lower and upper bounds define
353 on both edges the limited bandwidth, the most likely value indicates that values in the middle are more probable
354 than the boundary values, and also allows for the representation of skewness. The TPD is a popular distribution in
355 the risk analysis field (Cottin and Döhler, 2013) for example to reproduce expert estimates. Especially if little or no
356 information about the actual distribution of the parameter or only an estimate of the additional variables to fit the
357 theoretical distribution is feasible, a best possible approximation can be achieved using the TPD. If there is no
358 representative empirical data available as a basis for risk prediction, complex analytical (theoretical) distributions,
359 which are harder to model and communicate, may not represent the reality better than a simple triangular
360 distribution (Sander, 2012).

361 2. Beta-PERT distribution (BPD)

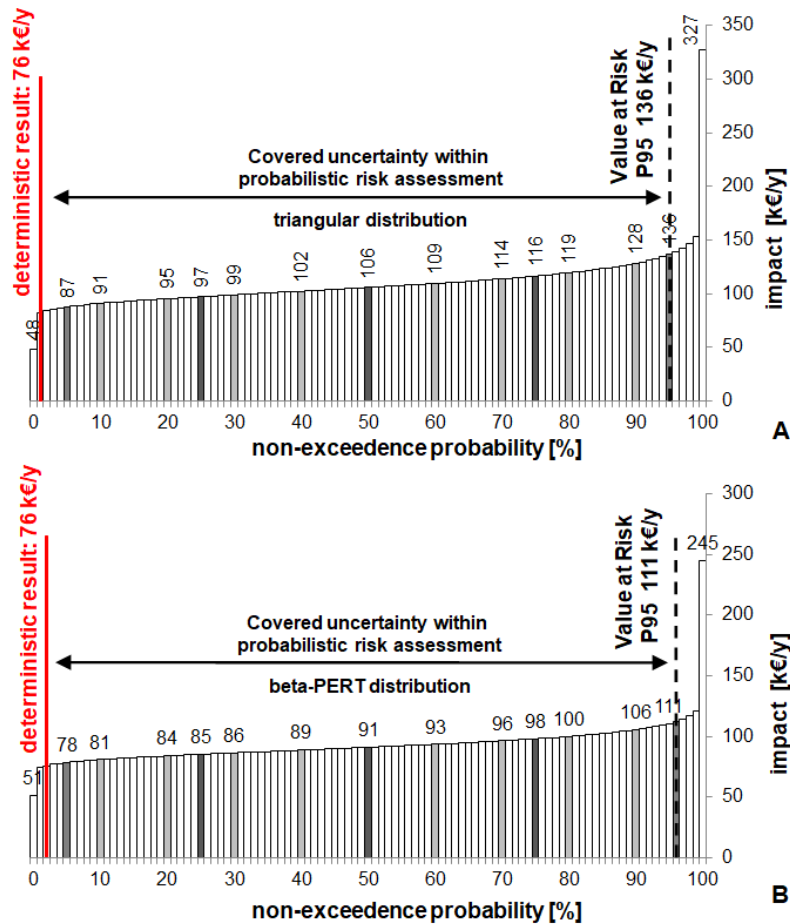
362 The beta-PERT distribution (Program Evaluation and Review Technique) is a simplification of the Beta
363 distribution with the advantage of an easier modelling and application (Sander, 2012). It requires the same three
364 parameters as a triangular distribution: l for lower bound, m for most likely value (mode) and u for upper bound. In
365 contrast to the two parametric normal distribution $N(\mu, \sigma)$ – μ for average and σ for standard deviation – the beta-
366 PERT distribution is limited on the edges and it allows for modelling asymmetric situations. Risk parameters
367 commonly have a natural boundary, for example vulnerability factors ranging from 0 (no loss) to 1 (total loss).
368 Therefore, estimating min/max values instead of standard deviation is more realistic or feasible as there is in most
369 cases no data available to express the mean variation. Moreover, BPD allows for smoother shapes, making it
370 suitable to model a distribution that is actually an aggregation of several other distributions.

371 For a given number of risks, each with a probability of occurrence and an individual probability distribution, the
372 potential number of combinations (scenarios) escalates nonlinear. Especially if dependencies or correlations between
373 different risks are included and/or numerous partial risks are aggregated to an overall risk the application of
374 analytical methods have computational restrictions. Stochastic simulations are better suited to work on such complex
375 models (Tecklenburg, 2003). Therefore, the aggregation of the distributions were calculated by means of Latin
376 Hypercube sampling (LHS) which is a comparable stochastic simulation technique to Monte-Carlo simulation
377 (MCS) with the advantage of a faster data processing, a better fitting on the theoretical input distribution and a more
378 efficiently calculation as fewer iterations are needed to get equally good results (Sander, 2012). LHS consistently
379 produces values for the distribution's statistics that are nearer to the theoretical values of the input distribution than
380 MCS. These advantages are possible because the real random numbers used to select samples for the MCS tend to
381 have local clusters, which are only averaged out for a very large number of draws. Addressing this issue using LHS
382 can immediately improve the quality of the result by splitting the probability distribution into n intervals of equal
383 probability, where n is the number of iterations that are to be performed on the model. In the present study, 1,000,000
384 iterations were performed for every single simulation to get consistent results.

385 5. Results and discussion

386 In Table 3 the results for each risk group (R_P , R_A , R_D) as well as for the total multi-hazard risk R_C calculated with the
387 standard deterministic risk approach are shown and compared to those obtained by the two probabilistic setups using
388 two different probability distributions (TPD and BPD). The results associated with the two distribution functions are
389 displayed as median value of the PDF to show their deviation to the outcome of the standard approach. Based on our
390 case study, the road risk over all hazards types and scenarios (multi-hazard risk) with the deterministic approach
391 results in 76.0 k€/y. The results with the probabilistic approach referring to the median of the PDFs amounts to a
392 monetary risk of 105.6 k€/y (TPD) and 90.9 k€/y (BPD), respectively. Compared to the standard approach the
393 median of the PDFs equals an increase of 38 % (BPD) and 19 % (TPD), depending on the choice of probability
394 distribution to model the uncertainties of the input variables. Focusing on the 95 % percentile (P95) of the results –
395 non-exceedance probability of 95 %, shown in Fig. 3 – an increase of 79 % (TPD) and 46 % (BDP) to the
396 deterministic result can be observed. Fig. 3 illustrates, based on the Lorenz curves for the two distributions (TPD and
397 BPD), the scale of deviation of the total multi-hazard risk R_C within the probabilistic risk modelling and compared to
398 the standard outcome. The graphs show the potential uncertainties of the risk computation, which can be covered by

399 a suitable choice of a Value at Risk (VaR) level. For example, with a benchmark of the 95 % quantile (P95), 95 % of
 400 the potential uncertainties within the risk calculation can be covered by using a probabilistic risk assessment
 401 approach. However, a suitable VaR level is depended on the general safety requirement of the system as well as on
 402 the degree of uncertainty of the input variables.



403
 404 **Figure 3.** Lorenz curves for (A) triangular distribution and (B) beta-PERT distribution showing the scale of
 405 deviation of the total multi-hazard risk R_C within the probabilistic risk modelling and compared to the deterministic
 406 result in k€/y.

407 Geological hazards (rockfall) contribute with a fraction of 7.8 % to the total risk (or, in absolute numbers, 5.9 k€, see
 408 Table 3) based on the deterministic model, which can be attributed to the relatively small importance in comparison
 409 to the other hazard types in the study area. Hydrological hazards pose the highest risk (50.5 %, or, in absolute
 410 numbers, 38.4 k€/y) previous to avalanche hazards (41.7 %, or, in absolute numbers, 31.7 k€/y). Overall, R_P (44.9 %;
 411 34.1 k€/y) has the highest share on the total multi-hazard risk narrowly followed by R_A (38.9 %; 29.6 k€/y), both
 412 associated to direct damage. The hydrological hazards (predominantly debris flow processes) with a portion of
 413 76.5 % or 26.1 k€/y have a disproportionate high share on R_P due to the high-intensity hazard impact. Similarly, the
 414 semi-empirical lethality factors shown in Table A7 have high values ($\lambda_D = 0.8$) just like the impact of rock fall on
 415 cars with a probability of death of $\lambda_R = 1.0$. Thus, these event types yield in high monetary losses in contrast to snow
 416 avalanches with a lethality factor for high intensity of $\lambda_A = 0.2$. By modelling the hazard-specific lethality with

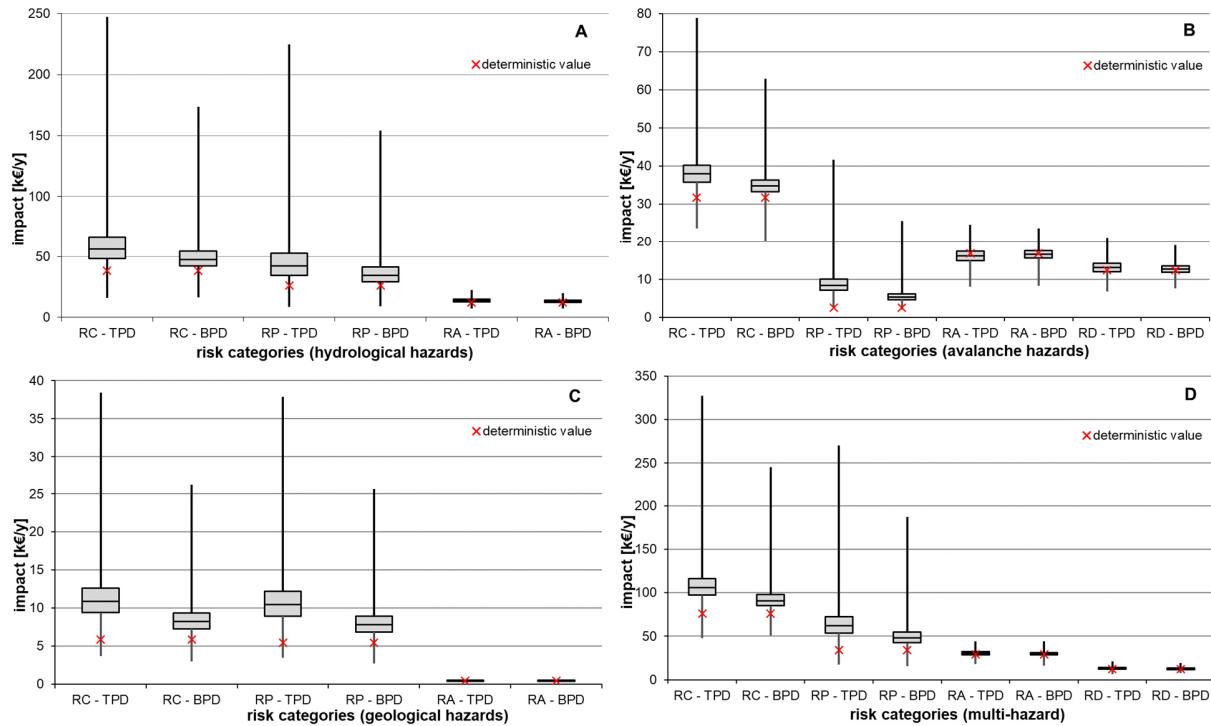
417 probability functions a wider scatter can be achieved but the effect still remains due to the heavy weight around the
 418 most likely value m . The indirect losses related to R_D with a fraction of 16.3 %, or, in absolute numbers 12.4 k€/y
 419 have a minor portion because this risk group is only relevant for snow avalanches.

420 **Table 3.** Comparison of the deterministic versus probabilistic results for the three risk categories depending on the
 421 three hazard types and the total collective risk with R_P = risk for persons, R_A asset risk, R_D = disposability risk and R_C
 422 = total collective risk with absolute values in k€/y in the first row and as percentage in the second row. For the
 423 probabilistic data, the median value of the triangular Δ and the beta-PERT \wedge distribution functions are displayed.
 424 Note that, risk-based aggregated losses do not equal the sum of the sub-components because probabilistic metrics
 425 such as P50 are not additive. Thus, the computational sum as well as the percentage are slightly different.

Risk category		R_P			R_A			R_D			R_C		
Hazard type	Unit	Det.	Δ	\wedge	Det.	Δ	\wedge	Det.	Δ	\wedge	Det.	Δ	\wedge
Geological hazards	k€/y	5.4	10.5	7.8	0.47	0.43	0.44	0	0	0	5.9	10.9	8.3
	%	15.8	17.0	16.3	1.6	1.4	1.5	0	0	0	7.8	10.3	9.1
Hydrological hazards	k€/y	26.1	42.3	34.5	12.3	13.9	13.1	0	0	0	38.4	56.2	47.6
	%	76.5	68.3	71.9	41.6	45.6	43.5	0	0	0	50.5	53.2	52.4
Avalanche hazards	k€/y	2.6	8.4	5.3	16.8	16.2	16.6	12.4	13.1	12.7	31.7	37.9	34.7
	%	7.6	13.6	11.0	56.8	53.1	55.1	100	100	100	41.7	35.9	38.2
Total	k€/y	34.1	61.9	48.0	29.6	30.5	30.1	12.4	13.1	12.7	76.0	105.6	90.9
	%	44.9	58.6	52.8	38.9	28.9	33.1	16.3	12.4	14.0	100	100	100

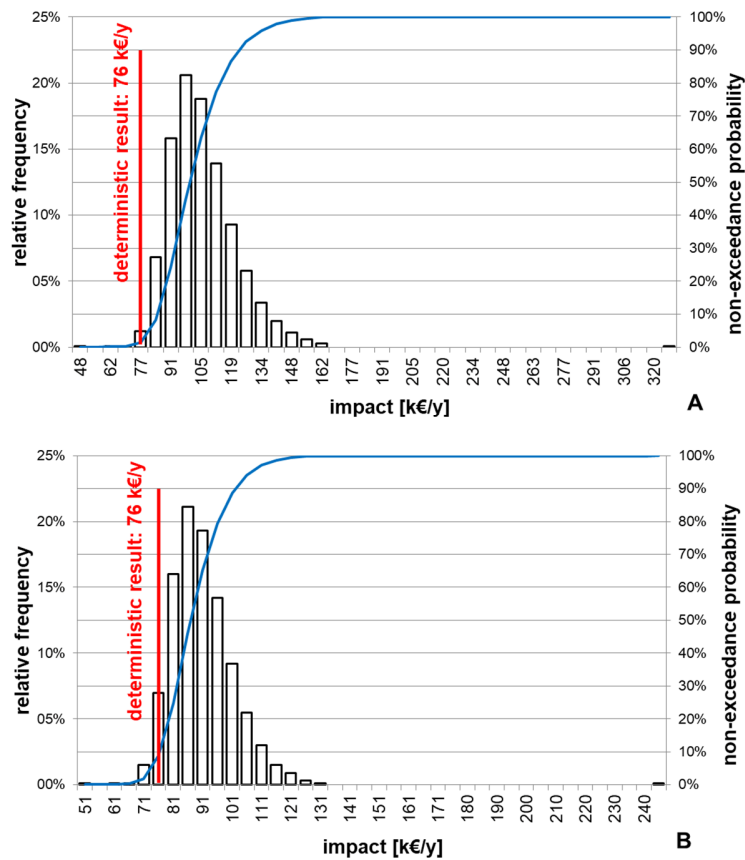
426 The results related to our case study (Table 3 and Fig. 4) show that due to the shape and the mathematical definition
 427 of the distribution the TPD leads to the highest variation in the monetary losses. The boxplots in Fig. 4 display the
 428 results from the probabilistic simulation for the three risk categories (R_P , R_A , R_D) and for the total hazard-specific risk
 429 (R_C) relating to the three hazard types (Figs. 3 A – C) and for the total multi-hazard collective risk (Fig. 4 D) in
 430 respect of the measures of the central tendency of the PDF. The boxplot diagrams are thereby plotted against the
 431 deterministic value to show its position. The wide range of the distribution in R_C is markedly caused by R_P , which
 432 exhibits a broad bandwidth and a right-skewed distribution. Hence, unlike to R_A and R_D , the physical injuries
 433 expressed as the economic losses of persons (R_P) are responsible for the highest divergence to the standard approach
 434 and show a considerable scatter. The main causes for the striking deviations can be associated to the relatively high
 435 monetary value of persons which was modelled as discrete point value in combination with the fluctuations of the
 436 MDT and the variations of the hazard specific lethality. The monetized costs for a statistical human life equal 3 M€
 437 (Table A7) and is based on a statistical survey of the economic expenses for a road accident in Austria (BMVIT,
 438 2014). Although we ascribe this value to a high degree of uncertainty the valuation of the expenses for a statistical
 439 human life was not attributed to a probability distribution due to the case study-specific fixed governmental
 440 requirements in Austria. The discussion of a monetarily evaluation of a human life is still ongoing across scientific
 441 disciplines using different economic approaches (e.g. Hood, 2017). Furthermore, the lethality factors also correspond
 442 to the high variation of R_P which are seen as very sensitive parameters. Therefore, we encourage further research on

443 hazard-specific lethality functions for road risk management either based on comprehensive empirical datasets or on
 444 representative hazard impact modelling. Due to the strong effect of R_P on R_C the results have to be carefully
 445 interpreted as they are sensitive to the input variables. Therefore, the values on our case study especially the cost for
 446 human life cannot be directly transferred to other application without a detailed validation and verification of
 447 national regulations.



448
 449 **Figure 4.** Probabilistic results for the three risk categories per hazard type (A = torrent processes, B = snow
 450 avalanches, C = rockfall) and for the total collective risk (D) based on the two distribution functions triangular or
 451 three-point distribution (TPD) and the beta-PERT distribution (BPD) with R_P = risk for persons, R_A asset risk, R_D =
 452 disposability risk and R_C = total collective risk in k€/year.

453 Apart from R_P where the deterministic result is located below or near the 5 % percentile of both PDFs, R_A and R_D are
 454 mostly within the interquartile range between the 25 % quartile and the median compared to the standard approach
 455 (Fig. 4). In this context, R_A for snow avalanche exceeds the median and is situated between the median and the 75 %
 456 quartile. The effect can be traced back to the left-skewed distribution of the vulnerability factor $v_{B,A}$ for medium
 457 avalanche hazard intensities regarding the object class structures (bridges and culverts) in Table A8. In general, due
 458 to the shape and the mathematical characteristics of the distribution, the BPD leads to a stronger compaction around
 459 the median than the TPD which can be well explained by the properties of the BPD which has, in comparison to the
 460 TPD, a larger weight around the most likely value m .



461
 462 **Figure 5.** Probability density function (PDF) and cumulative distribution function (CDF) for (A) triangular
 463 distribution, (B) beta-PERT distribution in k€/y.

464 In Fig. 5, the PDF and the cumulative distribution function (CDF) are shown for R_C with the two probabilistic model
 465 results and the deterministic result. In both cases (TPD and BPD), the deterministic result is situated at the lower
 466 edge of the PDF near or under the 5 % percentile. Thus, the deterministic result of our case study covers
 467 approximately less than 5 % of the potential band-width of the probability distribution. The TPD has a wide range,
 468 whereas the BPD is considerably flattened on the boundary of the amplitude. The results of the two distributions
 469 have in common that they are allocated right skewed. In contrast to the location of the median, the deterministic
 470 result is on the far-left side of both distribution and is exceeded of more than 95 % of the potential outcome.

471 **6 Conclusion**

472 The results based on our case study provide evidence that the monetary risk calculated with a standard deterministic
 473 method following the conventional guidelines is lower than applying a probabilistic approach. Thus, without
 474 consideration of uncertainty of the input variables risk might be underestimated using the operational standard risk
 475 assessment approach for road infrastructure. The mathematical product of the frequency of occurrence and the
 476 potential consequences with single values and, in a narrower sense, the multiplication of the partial risk factors in the

477 second part of the risk equation may lead to a bias in the risk magnitude because the multiplication of the ancillary
478 calculations generates a theoretical value ignoring the full scope of the total risk.

479 The far left position of the deterministic value within the PDF of the probabilistic result in our study can be traced
480 back to fact that the multiplication of two positive symmetrical distributions results in a right-skewed distribution,
481 because the product of the small numbers at the lower ends of the bandwidths results in much smaller numbers than
482 the product of the high numbers at the upper ends of the bandwidths. When right-skewed distributions are used as
483 input and aggregated, the effect of skewness shifts the deterministic value (represented by the most likely value) to
484 the right side of the resulting distribution. Even if conservative risk values are used in a deterministic setup, a
485 potential scatter (upper and lower bounds) remains, which leads within a probabilistic calculation through
486 aggregation of the partial risk elements and sub-results to a right-skewed distribution according to the skewness of
487 input variables. Since risk values of our study are in most cases asymmetric with primarily positive skews, the
488 deterministic result migrates during aggregation to the left side of the PDF in Fig. 5. The deterministic risk value is
489 usually expressed either as a theoretical mean value or as most likely value neglecting the potential distribution
490 functions of the input data. Thus, the compression of the input values to a single deterministic risk value with total
491 determination prevents an actual prognosis of reliability that would have been achieved by specifying bandwidths
492 (Sander, 2012). Furthermore, the simple summation of the scenario related and the object-based risk to receive the
493 cumulative risk level instead of using probabilistic risk aggregation leads to an underestimation of the final risk.
494 Hence, the full spectrum of risk cannot be represented with deterministic risk assessment, which may further lead to
495 biased decisions on risk mitigation.

496 The Value at Risk (VaR) approach by considering a reliable percentile of the non-exceedance probability e.g. P95 as
497 shown in Fig. 3 – depending on the desired covering of the risk potential from society, authorities or organizations –
498 might be an appropriate concept to tackle this challenge. In this context, a higher VaR value implies a higher safety
499 level for the system under investigation. The final results of risk assessments are subject to uncertainties mainly due
500 to insufficient data basis of input variables, which can be addressed using a PDF to represent uncertainties involved.
501 For further decisions on the realization of mitigation measures a high VaR value such as P95 covers these
502 uncertainties with a defined shortfall probability and thus supports decision makers with more information of road
503 risk. In turn, as a further practical improvement this benchmark can be compared to the same grade of safety for the
504 costs of mitigation measures since cost assessments for defence structures are also subject to considerable
505 uncertainties. Thus, an optimal risk-based design of defence structures might encompass a balance between the same
506 VaR level both of a probabilistic risk and a probabilistic cost assessment utilizing a cost benefit analysis (CBA).
507 However, within a probabilistic approach the scale of deviation is dependent on the choice of distribution for
508 modelling the bandwidth of the variables and the results are sensitive to the defined spectrum of input information
509 stated in Tables A6 - A9. These variables are case study specific and cannot be directly transferred to other road risk
510 assessments without careful validation. However, probabilistic risk assessment (PRA) enables a transparent
511 representation of potential losses due to the explicit consideration of the entire potential bandwidth of the variables
512 contributing to risk. Since comparable results can be achieved based on predefined values (Bründl et al., 2009), we
513 still recommend the consideration of the deterministic value as a comparative value to the probabilistic method.

514 Road risk assessment is usually afflicted to data scarcity; thus, risk operators and practitioners are often dependent on
515 expert appraisals, which are subject to uncertainties. In order to improve data quality, upper and lower values and the
516 expected value can be easily estimated for fitting a simple distribution of the input variables. Even though empirical
517 values such as statistical data are available, a certain degree of uncertainty remains. Therefore, simple distribution
518 functions such as TPD or BPD can adjust the shape of the distribution more conveniently than complex probability
519 distributions, since the required additional parameters to adjust a complex distribution are simple not available.
520 Hence, for a prognostic prediction, risk modelling with complex distributions in contrast to simple techniques cannot
521 be justified if there is a lack of empirical data.

522 A limitation of our study is that the performance of the probabilistic approach cannot be verified and validated with
523 empirical data, but the results show that the explicit inclusion of epistemic uncertainty leads to a bias in risk
524 magnitude. The probabilistic approach allows quantification of uncertainty, and thus enables decision makers to
525 better assess the quality and validity of the results from road risk assessments. This can facilitate the improvement of
526 road-safety guidelines (for example by implementing a VaR concept), and thus is of particular importance for
527 authorities responsible for operational road-safety, for design engineers and for policy makers due to a general
528 increase of information for optimal decision-making under budget constraints. Furthermore, the paper addresses the
529 second part of the risk concept in terms of the consequence analysis. The results of the hazard analysis serve thereby
530 as a constant input using the physical modelling of the hazard processes without the consideration of probabilistic
531 methods. Thus, the probability of occurrence of the hazard processes was mathematically processed as point value
532 within the probabilistic design since the hazard analyses (with deterministic design events to assess the hazard
533 intensities as a function of the return interval) was part of prior technical studies. Further considerations of a
534 probabilistic modelling of the frequency of the events were outside of the study design and might be addresses in
535 subsequent studies. Therefore, we expect a considerable source of epistemic uncertainty within the hazard analysis
536 which emphasises the necessity for an additional inclusion of probabilistic based hazard analyses in a holistic multi-
537 hazard risk environment. Even though the presented methodology in this study focuses on a road segment exposed to
538 a multi-hazard environment on a local-scale, the approach can easily be transferred to other risk-oriented purposes.

539
540 *Acknowledgments:* This work was supported by the Federal State government of Salzburg, Austria, especially from
541 the Geological Service under supervision of L. Fegerl and G. Valentin. The geological hazard analysis was
542 conducted by Geoconsult ZT-GmbH by A. Schober on behalf of the Federal State government of Salzburg which
543 provided the hazard data for the risk analysis. The authors were supported by BOKU Vienna Open Access
544 Publishing Fund.

545 *Competing interests:* Sven Fuchs is member of the Editorial Board of Natural Hazards and Earth System Sciences.

546 *Author contribution:* SO initiated the research, was responsible for data collection, literature research, preparation of
547 the manuscript, visualization of the results and performed the risk simulations with additional contribution by PS. PS
548 contributed to additional information on probabilistic risk calculation. SF compiled the background on risk
549 assessment and helped to shape the research, analysis and the manuscript. All authors discussed the results and
550 contributed to the final manuscript.

551 *Data availability:* All risk related data are publicly available (see references throughout the paper as well as in the
552 Appendix).
553

554 **Appendix**

555 **Risk equations according to ASTRA (2012) guideline:**

556 A. Risk for persons R_P

557 1. Direct impact of the hazard event – standard situation

558
$$r_{(DI)NS,j} = p_j \times (1 - p_{Rb}) \times (1 - p_{RbE}) \times p_N \times N_P \times \lambda \times p_{So,j} \times f_L \quad (1A)$$

559 **Table A1.** Risk variables and their derivation for the calculation of R_P – direct impact standard situation. (*)The
 560 reduction factor considers that not all hazard areas get simultaneously released by the same triggering event. (#)The
 561 number of hazard areas for the three hazard types was calculated as discrete values based on field surveys according
 562 to the release probability as a function of the event frequency (avalanches $n_{A10} = 6$, $n_{A30} = 7$; torrent processes n_{T10}
 563 $= 7$, $n_{T30} = 8$; rockfall $p_{RbE} = 0$ not relevant). (x)The length of the affected street segment is a discrete (single) value
 564 according to the results of the hazard analyses.

Variable	Description	Derivation
$r_{(DI)NS,j}$	risk of persons in scenario j (normal situation)	
p_j	probability of occurrence of an event (frequency of a scenario j)	$p_j = f_j - f_{j+1}; f_j = \frac{1}{T_j}$ p_j = probability of occurrence of scenario j f_j = frequency of occurrence T_j = return period of scenario j
p_{Rb}	probability of precautionary road blockage	
p_{RbE}	probability of a road blockage due to an event (road closure due to a previous event of the same hazard type along the road)	$p_{RbE} = \alpha \times \left(1 - \frac{1}{n_H}\right)$ α = reduction factor(*) n_H = number of hazard areas with the same hazard process and triggering mechanism(#)
p_N	probability of the standard (normal) situation	$p_N = 1 - p_C$
p_C	probability of a traffic jam (congestion)	$p_C = \left(\frac{n}{365}\right) \times \left(\frac{D}{24}\right)$ n = number of traffic jams per year D = average duration of a traffic jam [h]
N_P	number of affected persons	$N_P = N_V \times \beta$ $N_{VN} = \frac{MDT}{v \times 24000} \times l = \text{number of vehicles in the standard situation}$ $N_{VJ} = \frac{(\rho_{max} \times l)}{1000} = \text{number of vehicles in case of a traffic jam}$ MDT = mean daily traffic v = signalized velocity for cars [km/h] l = length of the street segment [m] ^(x) ρ_{max} = maximum traffic density per lane and kilometer in case of a traffic jam β = mean degree of passengers
λ	lethality factor	Hazard-process and intensity related variable ($\lambda_D, \lambda_F, \lambda_R, \lambda_A$ in table A6)
$p_{So,j}$	spatial occurrence probability of the	for rockfall processes $p_{So,j} = ET \times \frac{d}{w_{HD}}$

	process in the scenario j as proportion of the mean width or area of the process domain in scenario j to the maximum width or area of the potential hazard domain	ET = event type d = mean diameter of the block [m] w_{HD} = width or amplitude of the hazard domain in scenario j
f_L	factor to differentiate the affected lane	0,5 = one lane affected 1 = whole road (both lanes) affected

565 2. Direct impact of the hazard event – special situation due to traffic jam

$$566 \quad r_{(DI)SS,j} = p_j \times (1 - p_{Rb}) \times (1 - p_{RbE}) \times p_C \times N_P \times \lambda \times p_{So,j} \times f_L \quad (2A)$$

567 **Table A2.** Risk of persons in scenario j for the calculation of R_P – direct impact traffic jam. The calculation of the
568 variables is according to Table A1.

Variable	Description
$r_{(DI)SS,j}$	risk of persons in scenario j in case of a traffic jam (special situation)

569 3. Indirect effect – Rear-end collision

$$570 \quad r_{(RC)NS,j} = p_j \times (1 - p_{Rb}) \times (1 - p_{RbE}) \times p_{Rc} \times f_L \times (1 - p_C) \times N_P \times \lambda_{Rc} \quad (3A)$$

571 **Table A3.** Risk variables and their description for the calculation of R_P – rear-end collision. The calculation of the
572 residual variables is according to Table A1. (*)A rear-end collision is only valid in case of a standard situation (no
573 traffic jam). The scenario is not relevant for low intensity hazard events with deposition heights < 0,15 m.

Variable	Description
$r_{(RC)NS,j}$	risk of persons in scenario j for a rear-end collision in the normal situation(*)
p_{Rc}	probability of rear-end collision
λ_{Rc}	probability of fatality in the case of a rear-end collision

574 B. Property risk R_A

$$575 \quad r_{(DI)i,j} = p_j \times l \times A_i \times v_{i,j} \times p_{So,j} \times f_L \quad (4A)$$

576 **Table A4.** Risk variables and their description for the calculation of R_A – direct impact. The calculation of the
577 residual variables is according to Table A1.

Variable	Description
$r_{(DI)i,j}$	risk of object i in scenario j in terms of a direct impact of the hazard
A_i	asset value of object i
$v_{i,j}$	hazard-specific vulnerability of object i in scenario j (in table A7)
l	length of the affected road segment

578

579 C. Risk due to non-operational availability R_D

$$580 \quad r_{Rb,j} = \left(p_j \times f_{Rb} \times \frac{1}{n_H} \right) \times D_{Rb} \times C_{Rb} \quad (5A)$$

581 **Table A5.** Risk variables and their description for the calculation of R_D . The calculation of the residual variables is
 582 according to Table A1.

Variable	Description
$r_{Rb,j}$	risk of a roadblock in scenario j
f_{Rb}	frequency of road blockage
D_{Rb}	duration of road blockage depended on the hazard type
C_{Rb}	costs of a road blockage
n_H	number of hazard areas which are responsible for road closure

583 **Risk variables:**

584 A. Probability of loss – exposure

585 **Table A6.** Band width (credible intervals with l - lower bound, m - most likely value and u - upper bound) of the
 586 variables within the probabilistic risk analysis for calculating exposure situations. Units: h for hours, n for numbers,
 587 y for years. (*)Event type 1|5|10 equates to single stone | multiple stones | small scale rockslide.

Variable	Description	Specification	Unit	l - lower bound	m - most likely value	u - upper bound	Source
p_{Rb}	probability of a roadblock	not probable	-	0			m: ASTRA (2012); l, u: Estimates considering ASTRA class limits
		sparse probable		0.05	0.1	0.5	
		probable		0.1	0.5	0.9	
		most likely		0.5	0.9	0.95	
α	reduction factor for p_{RbE}	--	-	0.5	0.75	1	m: ASTRA (2012); l, u: Expert judgements
n_{B99}	number of traffic jams per year	--	n/y	0	1	2	l, m, u: Expert judgements icw. surveyor of highways (Federal State of Salzburg)
D	duration of a traffic jam	--	h	0.083	0.5	2.0	l, m, u: Expert judgements icw. surveyor of highways (Federal State of Salzburg)
f_{A10}	frequency of occurrence special situation A10	--	n/y	5	22	30	l, m, u: Statistical evaluation traffic jam database ASFINAG for the year 2015 (min., mean, max. value)

D_{A10}	duration of a special situation A10	--	h	0.5	2.65	5.0	l, m, u: Statistical evaluation traffic jam database ASFINAG for the year 2015 (min., mean, max. value)
n_{SS}	number of traffic jams in case of a special situation A10	--	n	0	4	11	l, m, u: Statistical evaluation traffic jam database ASFINAG for the year 2015 traffic jam events > 0.5h
D_{A10}	duration of a traffic jam special situation A10	--	h	0.083	1	2	l, m, u: Statistical evaluation traffic jam database ASFINAG for the year 2015
p_{RC}	Probability of a rear-end collision	improbable	-	0	0.05	0.15	m: ASTRA (2012); l, u: Estimates considering ASTRA class limits
		medium probable		0.05	0.15	0.25	
		frequent		0.15	0.25	0.35	
ET	event type of rock fall ^(*)	--	-	1	5	5	ASTRA (2012) icw. geological expert judgement

588 D. Degree of damage – Risk for persons R_p

589 **Table A7.** Band width (credible intervals l - lower bound, m - most likely value and u - upper bound) of the variables
590 within the probabilistic risk analysis for calculating R_p . Units: h for hours, n for numbers. ^(*)The monetary value of
591 person was used as single (point) value as this value is recommended from the Austrian government.

Variable	Description	Specific-ation	Unit	l - lower bound	m - most likely value	u - upper bound	Source
λ_{RC}	probability of fatality in the case of a rear-end collision	--	-	0	0.0066	0.05	m: ASTRA (2012); l, u: Expert judgements icw. surveyor of highways (Federal State of Salzburg)
λ_D	lethality for debris flow	low intensity	-	0			m: ASTRA (2012) and BAFU (2013); l, u: Estimates considering class limits
		medium intensity		0	0.5005	0.7995	
		strong intensity		0.5005	0.7995	1	
λ_F	lethality for dynamic flooding	low intensity	-	0			m: ASTRA (2012) and BAFU (2013); l, u: Estimates considering class limits
		medium intensity		0	0.0025	0.108	
		strong intensity		0.025	0.108	0.20	
λ_R	lethality for rock fall	low intensity	-	0	0.1	0.8	m: ASTRA (2012) and BAFU (2013) l, u: Estimates considering class limits
		medium intensity		0.1	0.8	1	

		strong intensity		0.8	1	1	
λ_A	lethality for avalanche	low intensity	-	0	0.00025	0.1	m: ASTRA (2012) and BAFU (2013); l, u: Estimates considering class limits
		medium intensity		0.00025	0.1	0.2	
		strong intensity		0.1	0.2	1	
MDT _{B99}	Average daily traffic B99	--	n	3.000	3.600	7.000	l, m, u: Traffic counting for the year 2016 (min., mean, max. value) (Federal State of Salzburg)
MDT _{A10}	average daily traffic A10	--	n	10.000	19.638	62.000	l, m, u: Permanent automatic traffic counting ASFINAG for the year 2016 (min., mean, max. value)
v	signalized velocity for cars	free land zone	km/h	80	100	120	m: signalized travel speed; l, u: Expert judgements icw. surveyor of highway (Federal State of Salzburg)
		municipality zone	km/h	45	50	60	
		acceleration / deceleration	km/h	70	80	110	
ρ_{max}	maximum traffic density per lane and kilometer in case of a traffic jam	--	n	120	140	145	m: ASTRA (2012); l, u: Expert judgements icw. surveyor of highway (Federal State of Salzburg)
β	mean degree of passengers	--	n	1	1.76	5	m: ASTRA (2012); l, u: Estimates considering one person (driver) and 5 persons in a car.
C_P	value (cost) of a person	--	€	3,016,194 ^(*)			BMVIT (2014) for the period 2014-2016

592 E. Extent of damage – Risk for material assets R_A

593 **Table A8.** Band width (credible intervals l - lower bound, m - most likely value and u - upper bound) of the variables
594 within the probabilistic risk analysis for calculating R_A . ^(*)Base value according to the Federal State of Salzburg:
595 $l = - 20 \%$, $u = + 10 \%$ (right-skewed distribution).

Variable	Description	Specification	Unit	l - lower bound	m - most likely value	u - upper bound	Source
A_R	asset value – construction costs road	--	€/m	800	850	1,000	l, m, u: Statistical data from Federal State of Salzburg (min., mean, max. value)

A_B	asset value – construction costs bridges (span with 8-10m)	--	€/m ²	1,350	2,200	2,400	l, m, u: Statistical data from Federal State of Salzburg (min., mean, max. value)
A_C	asset value – construction costs pipe culverts DN 500-1200	--	k€	52	65	71.5 ^(*)	m: Statistical data from Federal State of Salzburg l = - 20 %; u = + 10 % (right-skewed distribution)
$v_{R,F}$	vulnerability road dynamic flooding	low intensity	-	0	0.05	0.1	m: ASTRA (2012) and BAFU (2013); l. u: Estimates considering class limits
		medium intensity		0.05	0.1	0.45	
		strong intensity		0.1	0.45	0.80	
$v_{B,F}$	vulnerability structures (bridges) dynamic	low intensity	-	0	0.025	0.05	m: ASTRA (2012) and BAFU (2013); l. u: Estimates considering class limits
		medium intensity		0.025	0.05	0.65	
		strong intensity		0.05	0.65	1	
$v_{R,D}$	vulnerability road debris flow	low intensity	-	0	0.05	0.35	m: ASTRA (2012) and BAFU (2013); l. u: Estimates considering class limits
		medium intensity		0.05	0.35	0.65	
		strong intensity		0.35	0.65	1	
$v_{B,D}$	vulnerability structures (bridges, culvert) debris flow	low intensity	-	0	0.025	0.25	m: ASTRA (2012) and BAFU (2013); l. u: Estimates considering class limits
		medium intensity		0.025	0.25	0.95	
		strong intensity		0.25	0.95	1	
$v_{R,A}$	vulnerability road avalanche	low intensity	-	0	0.005	0.1	m: ASTRA (2012) and BAFU (2013); l. u: Estimates considering class limits
		medium intensity		0.005	0.1	0.2	
		strong intensity		0.1	0.2	0.30	
$v_{B,A}$	vulnerability structures (bridges, culvert) avalanche	low intensity	-	0	0.005	0.7	m: ASTRA (2012) and BAFU (2013); l. u: Estimates considering class limits
		medium intensity		0.005	0.7	1	
		strong intensity		0.7	1	1	
$v_{R,R}$	vulnerability road rock fall	low intensity	-	0	0.1	0.5	m: ASTRA (2012) and BAFU (2013) l, u: Estimates considering class limits
		medium intensity		0.1	0.5	1	
		strong intensity		0.5	1	1	

$v_{B,R}$	vulnerability structures (bridges, culvert) rock fall	low intensity	-	0	0.1	0.5	m: ASTRA (2012) and BAFU (2013) l, u: Estimates considering class limits
		medium intensity		0.1	0.5	1	
		strong intensity		0.5	1	1	

596 B. Degree of damage – Risk for operational availability R_D

597 **Table A9.** Band width (credible intervals l - lower bound, m - most likely value and u - upper bound) of the variables
598 within the probabilistic risk analysis for calculating R_D . Units: d for days, n for numbers, y for years.

Variable	Description	Specification	Unit	l - lower bound	m - most likely value	u - upper bound	Source
f_{Rb}	frequency of road blockage	--	n/y	1	2	4	l, m, u: ASTRA (2012) icw. expert judgements (local avalanche commission)
$D_{Rb,A10}$	duration of a precautionary roadblock for avalanche with return interval T_{10}	--	d	0.33	1	2	l, m, u: ASTRA (2012) icw. expert judgements (local avalanche commission)
$D_{Rb,A30}$	duration of a precautionary roadblock for avalanches with return interval T_{30}	--	d	1	2	3	l, m, u: ASTRA (2012) icw. expert judgements (local avalanche commission)
$C_{Rb,W}$	expenses of a roadblock during winter season	--	M€	1.245	1.557	1.868	m: BMNT (2015) CBA with statistical data of guest-night per hotel category (local tourism agency, 2015) l, u; Range of fluctuation +/- 20 %

599

600 **References**

- 601 Apel, H., Thieken, A. H., Merz, B., Blöschl, G.: Flood risk assessment and associated uncertainty, *Nat. Hazards and*
602 *Earth Syst. Sci.*, 4, 295–308, <https://doi.org/10.5194/nhess-4-295-2004>, 2004.
- 603 Austrian Standards International: Protection works for torrent control – Terms and their definitions as well as
604 classification, ONR 24800:2009 02 15, Vienna, 2009.
- 605 Austrian Standards International: Permanent technical avalanche protection – Terms, definition, static and dynamic
606 load assumptions, ONR 24805:2010 06 01, Vienna, 2010.
- 607 Austrian Standards International: Technical protection against rockfall – Terms and definitions, effects of actions,
608 design, monitoring and maintenance, ONR 24810:2017 02 15, Vienna, 2010.
- 609 ASTRA: Naturgefahren auf Nationalstraßen: Risikokonzept, Methodik für eine risikobasierende Beurteilung,
610 Prävention und Bewältigung von gravitativen Naturgefahren auf Nationalstraßen V2.10, Bundesamt für Straßen
611 ASTRA, Bern, 2012.
- 612 Bell, R., Glade, T.: Quantitative risk analysis for landslides – Examples from Bildudalur, NW-Iceland, *Nat. Hazards*
613 *and Earth Syst. Sci.*, 4, 117-131, <https://doi.org/10.5194/nhess-4-117-2004>, 2004.
- 614 Benn, J. L.: Landslide events on the West Coast, South Island, 1867-2002, *New Zealand Geographer*, 61, 3-13,
615 <https://doi.org/10.1111/j.1745-7939.2005.00001.x>, 2005.
- 616 BMLFUW: Richtlinie für Gefahrenzonenplanung, 2011.
- 617 BMNT: Richtlinien für die Wirtschaftlichkeitsuntersuchung und Priorisierung von Maßnahmen der Wildbach- und
618 Lawinenverbauung (Kosten-Nutzen-Untersuchung), Vienna, available at: [https://www.bmnt.gv.at/forst/wildbach-](https://www.bmnt.gv.at/forst/wildbach-lawinenverbauung/richtliniensammlung/Richtlinien.html)
619 [lawinenverbauung/richtliniensammlung/Richtlinien.html](https://www.bmnt.gv.at/forst/wildbach-lawinenverbauung/richtliniensammlung/Richtlinien.html), (last access: 01 June 2016), 2015.
- 620 BMVIT: Durchschnittliche Unfallkosten Preisstand 2011, Bundesministerium für Verkehr, Innovation und
621 Technologie BMVIT, Vienna, available at:
622 <https://www.bmvit.gv.at/verkehr/strasse/sicherheit/strassenverkehrsunfaelle/ukr2012.html>. (last access: 01 June
623 2016), 2014.
- 624 Bründl M. (Ed.): Risikokonzept für Naturgefahren – Leitfaden. Nationale Plattform für Naturgefahren PLANAT,
625 Bern, 2009.
- 626 Bründl, M., Romang, H. E., Bischof, N., Rheinberger, C. M.: The risk concept and its application in natural hazard
627 risk management in Switzerland, *Nat. Hazards Earth Syst. Sci.*, 9, 801–813, [https://doi.org/10.5194/nhess-9-801-](https://doi.org/10.5194/nhess-9-801-2009)
628 [2009](https://doi.org/10.5194/nhess-9-801-2009), 2009.
- 629 Bründl, M., Bartelt, P., Schweizer, J., Keiler, M., Glade, T.: Review and future challenges in snow avalanche risk
630 analysis, In: Alcántara-Ayala, I., Goudie, A. S. (Eds.), *Geomorphological Hazards and Disaster Prevention*,
631 Cambridge University Press 2010, pp 49-61, 2010.
- 632 Bründl, M., Ettl, L., Burkard, A., Oggier, N., Dolf, F. und Gutwein, P.: *EconoMe – Wirksamkeit und*
633 *Wirtschaftlichkeit von Schutzmaßnahmen gegen Naturgefahren, Formelsammlung*, 2015.
- 634 Bundesamt für Umwelt BAFU (2013): Objektparameterliste EconoMe 2.2, Bern, 2013.
- 635 Bunce, C., Cruden, D., Morgenstern, N.: Assessment of the hazard from rock fall on a highway, *Canadian*
636 *Geotechnical Journal*, 34, 344-356, <https://doi.org/10.1139/t97-009>, 1997.

637 Ciurean, R. L., Hussin, H., van Westen, C. J., Jaboyedoff, M., Nicolet, P., Chen, L., Frigerio, S., Glade, T.: Multi-
638 scale debris flow vulnerability assessment and direct loss estimation of buildings in the Eastern Italian Alps, *Nat.*
639 *Hazards*, 85, 929-957, <https://doi.org/10.1007/s11069-016-2612-6>, 2017.

640 Cottin, C., Döhler, S.: Risikoanalyse. Modellierung, Beurteilung und Management von Risiken mit Praxisbeispielen,
641 Studienbücher Wirtschaftsmathematik, 2. Auflage, Springer Spektrum, Wiesbaden, <https://doi.org/10.1007/978-3-658-00830-7>, 2013.

643 Dai, E.C., Lee, C.F., Ngai, Y.Y.: Landslide risk assessment and management: an overview, *Eng. Geol.*, 64, 65-87,
644 [https://doi.org/10.1016/S0013-7952\(01\)00093-X](https://doi.org/10.1016/S0013-7952(01)00093-X), 2002.

645 Dorren, L. K. A.: Rockyfor3D (V5.1) Transparent description of the complete 3D rockfall model, ecorisQ Paper,
646 <https://www.ecorisq.com>, 2012.

647 Fell, R., Corominas, J., Bonnard, C., Cascini, L., Leroi, E., Savage, W.: Guidelines for landslide susceptibility,
648 hazard and risk zoning for land-use planning, *Eng. Geol.*, 102 (3-4), 85-98,
649 <https://doi.org/10.1016/j.enggeo.2008.03.022>, 2008a.

650 Fell, R., Corominas, J., Bonnard, C., Cascini, L., Leroi, E., Savage, W.: Guidelines for landslide susceptibility,
651 hazard and risk zoning for land-use planning – Commentary, *Eng. Geol.*, 102 (3-4), 99-111,
652 <https://doi.org/10.1016/j.enggeo.2008.03.014>, 2008b.

653 Ferlisi, S., Cascini, L., Corominas, J., Matano, F.: Rockfall risk assessment to persons travelling in vehicles along a
654 road: the case study of the Amalfi coastal road (southern Italy), *Nat. Hazards*, 62, 691-721,
655 <https://doi.org/10.1111/nzg.12170>, 2012.

656 Flow-2D Software: Flow-2D Reference Manual, Nutrioso, 2017.

657 Fuchs, S., Heiss, K., Hübl, J.: Towards an empirical vulnerability function for use in debris flow risk assessment,
658 *Nat. Hazards and Earth Syst. Sci.*, 7, 495–506, <https://doi.org/10.5194/nhess-7-495-2007>, 2007.

659 Fuchs, S.: Susceptibility versus resilience to mountain hazards in Austria – paradigms of vulnerability revisited, *Nat.*
660 *Hazards and Earth Syst. Sci.*, 9, 337-352, <https://doi.org/10.5194/nhess-9-337-2009>, 2009.

661 Fuchs, S., Keiler, M., Sokratov, S., Shnyparkov, A.: Spatiotemporal dynamics: the need for an innovative approach
662 in mountain hazard risk management, *Nat. Hazards*, 68, 1217-1241, <https://doi.org/10.1007/s11069-012-0508-7>,
663 2013.

664 Fuchs, S., Keiler, M., Zischg, A.: A spatiotemporal multi hazard exposure assessment based on property data, *Nat.*
665 *Hazards and Earth Syst. Sci.*, 15, 2127-2142, <https://doi.org/10.5194/nhess-15-2127-2015>, 2015.

666 Fuchs, S., Röthlisberger, V., Thaler, T., Zischg, A., and Keiler, M.: Natural hazard management from a
667 coevolutionary perspective: Exposure and policy response in the European Alps, *Annals of the American*
668 *Association of Geographers*, 107, 382-392, <https://doi.org/10.1080/24694452.2016.1235494>, 2017.

669 Fuchs, S., Keiler, M., Ortlepp, R., Schinke, R., Papathoma-Köhle, M.: Recent advances in vulnerability assessment
670 for the built environment exposed to torrential hazards: Challenges and the way forward, *J. Hydrol.*, 575, 587-595,
671 <https://doi.org/10.1016/j.jhydrol.2019.05.067>, 2019.

672 Geoconsult ZT GmbH: Gefahrenanalyse B99, Technischer Bericht Sturzprozesse, Salzburg, 2016.

673 Grêt-Regamey, A., Straub, D.: Spatially explicit avalanche risk assessment linking Bayesian networks to a GIS, *Nat.*
674 *Hazards Earth Syst. Sci.*, 6, 911–926, <https://doi.org/10.5194/nhess-6-911-2006>, 2006.

675 Guikema, S., McLay, L., Lambert, J. H.: Infrastructure Systems, Risk Analysis, and Resilience - Research Gaps and
676 Opportunities, *Risk Anal.*, 35 (4), 560-561, <https://doi.org/10.1111/risa.12416>, 2015.

677 Hendrikx, J., Owens, I.: Modified avalanche risk equations to account for waiting traffic on avalanche prone roads,
678 *Cold Reg. Sci. and Technol.*, 51, 214-218, <https://doi.org/10.1016/j.coldregions.2007.04.011>, 2008.

679 Hood K.: The science of value: Economic expertise and the valuation of human life in US federal regulatory
680 agencies, *Soc. Stud. Sci.*, 47 (4), 441-465. <https://doi.org/10.1177/0306312717693465>, 2017.

681 Hungr, O., Beckie, R.: Assessment of the hazard from rock fall on a highway: Discussion, *Canadian Geotechnical*
682 *Journal*, 35, 409, <https://doi.org/10.1139/t98-002>, 1998.

683 International Organisation for Standardisation: Risk management – Principles and guidelines on implementation,
684 ISO 31000, Geneva, 2009.

685 IUGS Committee on Risk Assessment: Quantitative risk assessment for slopes and landslides – The state of the art,
686 In: Cruden, E.M., Fell, R. (Eds.), *Proceedings of the International Workshop of Landslide Risk Assessment*,
687 Honolulu, pp 3-12, 1997.

688 Kappes, M.S., Keiler, M., von Elverfeldt, K., Glade, T.: Challenges of analyzing multi-hazard risk: a review, *Nat.*
689 *Hazards*, 64, 1925-1958, <https://doi.org/10.1007/s11069-012-0294-2>, 2012a.

690 Kappes, M.S., Gruber, K., Frigerio, S., Bell, R., Keiler, M., Glade, T.: The MultiRISK platform: The technical
691 concept and application of a regional-scale multihazard exposure analysis tool, *Geomorphology*, 151-152, 139-155,
692 <https://doi.org/10.1016/j.geomorph.2012.01.024>, 2012b.

693 Kirchsteiger, C.: On the use of probabilistic and deterministic methods in risk analysis, *Journal of Loss Prevention in*
694 *the Process Industries*, 12, 399–419, [https://doi.org/10.1016/S0950-4230\(99\)00012-1](https://doi.org/10.1016/S0950-4230(99)00012-1), 1999.

695 Kristensen, K., Harbitz, C., Harbitz, A.: Road traffic and avalanches - methods for risk evaluation and risk
696 management, *Surveys in Geophysics*, 24, 603-616, <https://doi.org/10.1023/B:GEOP.0000006085.10702.cf>, 2003.

697 Lechowska, E.: What determines flood risk perception? A review of factors of flood risk perception and relations
698 between its basic elements *Natural Hazards*, 94, 1341-1366, <https://doi.org/10.1007/s11069-018-3480-z>, 2018 .

699 Margreth, S., Stoffel, L., Wilhelm, C.: Winter opening of high alpine pass roads - analysis and case studies from the
700 Swiss Alps, *Cold Reg. Sci. and Technol.*, 37, 467-482, [https://doi.org/10.1016/S0165-232X\(03\)00085-5](https://doi.org/10.1016/S0165-232X(03)00085-5), 2003.

701 Markantonis, V., Meyer, V., Schwarze, R.: Valuating the intangible effects of natural hazards – review and analysis
702 of the costing methods, *Nat. Hazards Earth Syst. Sci.*, 12, 1633–1640, [https://doi.org/10.5194/nhess-12-1633-](https://doi.org/10.5194/nhess-12-1633-2012)
703 2012, 2012.

704 Merz, B., Kreibich, H., Thielen, A. H., Schmidke, R.: Estimation uncertainty of direct monetary flood damage to
705 buildings, *Nat. Hazards Earth Syst. Sci.*, 4, 153–163, <https://doi.org/10.5194/nhess-4-153-2004>, 2004.

706 Merz, B., Elmer, F., Thielen, A. H.: Significance of “high probability/low damage” versus “low probability/high
707 damage” flood events, *Nat. Hazards Earth Syst. Sci.*, 9, 1033–1046, <https://doi.org/10.5194/nhess-9-1033-2009>,
708 2009.

709 Merz, B., Thielen, A. H.: Flood risk curves and associated uncertainty bounds, *Nat. Hazards*, 51, 437–458,
710 <https://doi.org/10.1007/s11069-009-9452-6>, 2009.

711 Merz, B., Thielen, A. H.: Separating natural and epistemic uncertainty in flood frequency analysis, *Journal of*
712 *Hydrology*, 309, 114–132, <https://doi.org/10.1016/j.jhydrol.2004.11.015>, 2005.

713 Merz, B., Kreibich, H., Schwarze, R., Thieken, A. H.: Assessment of economic flood damage, *Nat. Hazards Earth*
714 *Syst. Sci.*, 10, 1697–1724, <https://doi.org/10.5194/nhess-10-1697-2010>, 2010.

715 Meyer, V., Becker, N., Markantonis, V., Schwarze, R., van den Bergh, J. C. J. M., Bouwer, L. M., Bubeck, P.,
716 Ciavola, P., Genovese, E., Green, C., Hallegatte, S., Kreibich, H., Lequeux, Q., Logar, I., Papyrakis, E.,
717 Pfuerscheller, C., Poussin, J., Przyluski, V., Thieken, A. A., Viavattene, C.: Review article: Assessing the costs of
718 natural hazards – state of the art and knowledge gaps, *Nat. Hazards Earth Syst. Sci.*, 13, 1351-1373, [https://doi.org/](https://doi.org/10.5194/nhess-13-1351-2013)
719 [10.5194/nhess-13-1351-2013](https://doi.org/10.5194/nhess-13-1351-2013), 2013.

720 Michoud, C., Derron, M., Horton, P.: Rockfall hazard and risk assessments along roads at a regional scale: example
721 in Swiss Alps, *Nat. Hazards and Earth Syst. Sci.*, 12, 615-629, <https://doi.org/10.5194/nhess-12-615-2012>, 2012.

722 Oberndorfer, S., Fuchs, S., Rickenmann, D., Andrecs, P.: Vulnerabilitätsanalyse und monetäre Schadensbewertung
723 von Wildbachereignissen in Österreich, Bundesforschung- und Ausbildungszentrum für Wald, Naturgefahren und
724 Landschaft, BFW-Berichte, 139/2007, Wien, 2007.

725 Oberndorfer, S.: Technischer Bericht – Gefahrenanalyse Wildbach- & Lawinengefahren B99 Katschberg Straße,
726 Radstadt – Obertauern – Mauterndorf, km 24,70 – km 62,60, Leogang, 2016.

727 Rheinberger, C.M., Bründl, M., Rhyner, J.: Dealing with the white death: Avalanche risk management for traffic
728 routes, *Risk Anal.*, 29 (1), 76-94, <https://doi.org/10.1111/j.1539-6924.2008.01127.x>, 2009.

729 Republik Österreich: Forstgesetz 1975, BGBl 440/1975, Republik Österreich, Vienna, 1975.

730 Republik Österreich: Verordnung des Bundesministeriums für Land- und Forstwirtschaft vom 30. Juli 1976 über die
731 Gefahrenzonenpläne, BGBl 436/1975, Republik Österreich, Vienna, 1976.

732 Roberds, W.: Estimating temporal and spatial variability and vulnerability, In: Hungr, O., Fell, R., Couture, R. and
733 Eberhardt, E., (Eds.), *Landslide risk management*, Taylor and Francis Group, London, pp 129-157, 2005.

734 Schaerer, P.: The avalanche-hazard index, *Annals of Glaciology*, 13, 241-247, 1989.

735 Papathoma-Köhle, M., Kappes, M., Keiler, M., Glade, T.: Physical vulnerability assessment for alpine hazards: state
736 of the art and future needs, *Nat. Hazards*, 58, 645-680, <https://doi.org/10.1007/s11069-010-9632-4>, 2011.

737 Papathoma-Köhle, M., Gems, B., Sturm, M., Fuchs, S.: Matrices, curves and indicators: A review of approaches to
738 assess physical vulnerability to debris flow, *Earth-Sci. Rev.*, 171, 272-288,
739 <https://doi.org/10.1016/j.earscirev.2017.06.007>, 2017.

740 RiskConsult GmbH: RIAAT Risk Administration and Analysis Tools, Manual, Version 28-F01, Innsbruck, 2015.

741 Sander, P.: Probabilistische Risiko-Analyse für Bauprojekte. Entwicklung eines branchenorientierten
742 softwaregestützten Risiko-Analyse-Systems, University of Innsbruck, ISBN 978-3-902811-75-2, 2012.

743 Sander, P., Reilly, J.J. & Moergeli, A.: Quantitative Risk Analysis – Fallacy of the Single Number, ITA World
744 Tunnel Congress, 2015, Dubrovnik, 2015.

745 Sampl, P.: SamosAT – Beschreibung der Modelltheorie und Numerik, AVL List GmbH, Graz, 2007.

746 Schaub, Y., Bründl, M.: Zur Sensitivität der Risikoberechnung und Maßnahmenbewertung von Naturgefahren,
747 *Schweizerische Zeitschrift für Forstwesen*, 161(2), 27-35.

748 Schlögl, M., Richter, G., Avian, M., Thaler, T., Heiss, G., Lenz, G., Fuchs, S.: On the nexus between landslide
749 susceptibility and transport infrastructure – an agent-based approach, *Nat. Hazards and Earth Syst. Sci.*, 19 (1),
750 201-219, <https://doi.org/10.5194/nhess-19-201-2019>, 2019.

751 Straub, D., Grêt-Regamey, A.: A Bayesian probabilistic framework for avalanche modelling based on observation,
752 Cold Regions Science and Technology, 46, 192–203, https://doi.org/10.1007/978-3-319-09054-2_90, 2006.

753 Špačková, O., Rimböck, A., Straub, D.: Risk management in Bavarian Alpine torrents: a framework for flood risk
754 quantification accounting for subscenarios, in: Proc. of the IAEG Congress 2014, IAEG XII congress, Torino,
755 Italy, 2014.

756 Špačková, O.: RAT Risk Analysis Tool. Risk assessment and cost benefit analysis of risk mitigation strategies –
757 Methodology, Engineering Risk Analysis Group, Technical University of Munich, 2016.

758 Tecklenburg, T.: Risikomanagement bei der Akquisition von Großprojekten in der Bauwirtschaft, Dissertation, TU
759 Braunschweig, Schöling Verlag, Münster, 2003.

760 UNDRP: Natural disasters and vulnerability analysis, Department of Humanitarian Affairs/United Nations Disaster
761 Relief Office, Geneva, 1979.

762 UNISDR: Living with risk: A global review of disaster reduction initiatives, United Nations Publication, Geneva,
763 2004.

764 Unterrader, S., Almond, P., Fuchs, S.: Rockfall in the Port Hills of Christchurch: Seismic and non-seismic fatality
765 risk on roads. New Zealand Geographer, 74 (1), 3-14, <https://doi.org/10.1111/nzg.12170>, 2018.

766 Varnes, D.: Landslide hazard zonation: a review of principles and practice. UNESCO, Paris, 1984.

767 Wachinger, G., Renn, O., Begg, C., and Kuhlicke, C.: The risk perception paradox—implications for governance and
768 communication of natural hazards, Risk Anal., 33, 1049-1065, <https://doi.org/10.1111/j.1539-6924.2012.01942.x>,
769 2013.

770 Wastl, M., Stötter, J., Kleindienst, H.: Avalanche risk assessment for mountain roads: a case study from Iceland, Nat.
771 Hazards, 56, 465-480, <https://doi.org/10.1007/s11069-010-9703-6>, 2011.

772 Winter, B., Schneeberger, K., Huttenlau, M., Stötter, J.: Sources of uncertainty in a probabilistic flood risk model,
773 Nat. Hazards, 91, 431–446, <https://doi.org/10.1007/s11069-017-3135-5>, 2018.

774 Zischg, A., Fuchs, S., Keiler, M., Meissl, G.: Modelling the system behaviour of wet snow avalanches using an
775 expert system approach for risk management on high alpine traffic roads, Nat. Hazards and Earth Syst. Sci., 5, 821-
776 832, <https://doi.org/10.5194/nhess-5-821-2005>, 2005.